Research Article | Vol. 32, No. 23 / 4 Nov 2024 / Optics Express 41314
Optics EXPRESS

Determination of zooplankton absorption spectra and their potential contribution to ocean color

CAIT L. MCCARRY,[1,*] SÜNNJE L. BASEDOW,[2] EMLYN J. DAVIES,[3] KIM S. LAST,[4] AND DAVID MCKEE[1,2]

[1]Department of Physics, University of Strathclyde, Glasgow, Scotland, United Kingdom
[2]Department of Arctic and Marine Biology, UiT the Arctic University of Norway, Tromsø, Norway
[3]Department of Climate and Environment, SINTEF Ocean, Trondheim, Norway
[4]Scottish Association for Marine Sciences, Scottish Marine Institute, Oban, Scotland, United Kingdom
[*]cait.mccarry@strath.ac.uk

Abstract: Zooplankton are keystone organisms that provide a critical link between primary production and higher-order predators in the marine food web, as well as facilitating the sequestration of carbon within the ocean. In this context, there is considerable interest in the detection of zooplankton swarms from satellite ocean color signals. However, for this to be possible, accurate inherent optical property characterization of key zooplankton groups is first required. In this study, spectral absorption properties of six epipelagic zooplankton groups have been measured using what we believe to be a novel serial addition technique carried out with a Point Source Integrating Cavity Absorption Meter. The measured absorption spectra were used to model the impact of each group on remote sensing reflectance signals and determine a concentration threshold that would generate a distinguishable signal from ocean color data. Results indicate that the spectral shape of absorption did not vary much between species, with most organisms showing a peak at around 480 nm, characteristic of the pigment astaxanthin. Conversely, the magnitude of absorption did vary considerably between species, with larger organisms typically producing stronger absorption signals than smaller species. Thus, detection thresholds also varied for each group measured and were additionally influenced by background constituents within the water column. The calculated concentration thresholds indicate the feasibility of identifying zooplankton from ocean color, but owing to the spectral similarity in absorption properties, knowledge of *in situ* populations would be required to determine species abundances from satellite signals.

1. Introduction

Zooplankton are the heterotrophic component of the planktonic community and comprise a diverse group of organisms, ranging from 20 µm (microzooplankton) to 20 cm and greater in size (megazooplankton). They are a keystone group in the marine environment, owing to their sheer abundance and vital ecosystem roles. They represent an essential component of the marine food web, serving as an intermediary for the transfer of energy between primary producers (phytoplankton) and higher order predators, constituting the secondary and tertiary consumers. As a result, they directly support many commercially harvested species of fish and marine mammal species. Additionally, zooplankton themselves represent an important economic resource, as many species are regularly harvested for the production of aquaculture feed, as well as supplements for human consumption [1]. Furthermore, zooplankton are key regulators of the biological carbon pump, facilitating carbon capture and storage and allowing the ocean

#537062 https://doi.org/10.1364/OE.537062
Journal © 2024 Received 25 Jul 2024; revised 26 Sep 2024; accepted 16 Oct 2024; published 29 Oct 2024

Optics EXPRESS

to act as a critical buffer against the impacts of climate change [2,3]. As a result, they hold significant value and have been the focus of considerable scientific effort over the last century. Despite this, the 2001 Marine Zooplankton Colloquium stated that 'knowledge of their ecological function in their natural environment has increased only modestly' [4]. Traditional ship-based monitoring techniques likely contributed to this disparity between research effort and knowledge, as zooplankton populations are patchy by nature, making targeted sampling efforts challenging. In recent years, technology has advanced to allow for the development of more autonomous approaches to zooplankton sampling, including *in situ* imaging techniques such as Zooglider and Underwater Vertical Profiler, as well as static sensors attached to moorings (echo sounders, *in situ* cameras and holographic cameras). Whilst these approaches have increased our understanding of zooplankton dynamics, a 2023 review on monitoring marine zooplankton identified 'key knowledge and geographic gaps in monitoring coverage that need to be urgently addressed' [5].

Ocean color remote sensing signals are traditionally considered to be generated by mixtures of abundant yet relatively small particles (< 100 µm), including algal material and mineral suspended sediments (MSS), as well as colored dissolved organic materials (CDOM). As a result, extensive effort has been directed towards the optical characterisation of these constituents. However, a recent theoretical study by Davies et al. [6] demonstrated the possibility of larger (> 1 mm), less abundant particles (such as zooplankton), influencing the optical properties of the water column, especially absorption, if present in sufficient quantities (i.e. swarms). Further, in Basedow et al. [7] and McCarry et al. [8], it was demonstrated that surface swarms of the zooplankton *Calanus finmarchicus* could be identified from satellite imagery. The method developed in McCarry et al. used a standard Case-2 bio-optical model to identify regions of spectral anomaly associated with *C. finmarchicus*. With the addition of *C. finmarchicus* absorption into the model, optical closure was achieved and concentration estimates of *C. finmarchicus* were produced. In light of this work, it is possible that other important species of zooplankton may be detectable from ocean color signals, which could provide large-scale monitoring opportunities for these critical organisms. However, in order to achieve this, the inherent optical properties (IOPs) of these zooplankton groups require accurate characterisation.

IOP measurements of larger particles (such as zooplankton) have previously been a challenge, due to the bias of current measurement systems towards smaller particles. However, in the study conducted by Basedow [7], a method was developed to measure the spectral absorption properties of the zooplankton species *C. finmarchicus* using a Point Source Integrating Cavity Absorption Meter (PSICAM). The PSICAM has a cavity that holds nearly 400 ml of sample and measures absorption with a high degree of accuracy, free from scattering error. This makes the PSICAM ideal for measuring the absorption properties of particulate matter [9]. Following a serial addition methodology, live *C. finmarchicus* were sequentially added to the PSICAM to determine a per-individual absorption spectrum. This provides a method for the characterization of zooplankton absorption that can be utilized to measure other important species. Unfortunately, it is currently not possible to obtain complete IOP profiles for these organisms, as measurement biases do not allow the characterization of scattering and backscattering spectra for particles of this size class. However, Davies et al. [6] theoretically demonstrated that out of the water column IOPs, zooplankton are likely to most significantly contribute to absorption properties. This influence on absorption is especially apparent at the larger end of this group's size range (on the order of 10 mm and larger).

In this study, the spectral absorption properties of six different ecologically important zooplankton groups were measured in a PSICAM. Of these, five species belong to the Crustacean sub-phylum: the copepods *C. finmarchicus*, *Calanus hyperboreus* and *Paraeuchaeta norvegica,* as well as the Eumalacostraca species *Meganyctiphanes norvegica* (northern krill) and species from the genus *Parathemisto* (amphipods). All of these organisms have previously been recorded in near surface waters [10–15]. Crustaceans dominate the global zooplankton biomass, with

Optics EXPRESS

copepods representing the most abundant metazoan group of organisms on earth [16]. This means they play a critical role in the marine food web, acting as a vital link between primary production and higher order predators. Whilst often being partly transparent, the majority of these organisms are known to contain varying levels of carotenoid pigments, with the red pigment astaxanthin being the most prevalent. The exception to this is *Parathemisto*, which has more varied pigmentation and appears brown in color.

The antioxidant power of astaxanthin provides a variety of benefits for these organisms, including the protection of lipids from peroxidation and photoprotection from harmful solar radiation [17]. Despite this considerable role, color as a functional trait is largely overlooked in these organisms. This could be related in part to the practical limitations associated with the preservation of plankton samples in fixatives, which can lead to unreliable pigmentation information (due to oxidation or leaking). However, in a recent review of the role of astaxanthin in copepods, Vilgrain et al. [17] identified that coloration may be a key indicator of fitness, yielding important information on the health state of populations, as well as the transfer of antioxidants through trophic levels. Therefore, as well as understanding their impact on ocean color signals, measuring the live zooplankton absorption properties can inform understanding of the biology and potential health of these assemblages.

The final group measured in this study was the gastropod genus *Limacina* (sea butterflies). These are an abundant group of organisms with calcium carbonate shells of aragonite and dark pigmentation, which appears brown in color. Due to their abundance and calcium carbonate shells, these organisms play an important role in the carbonate pump in polar environments and are a good indicator species for ocean acidification [18].

The primary objective of this research was to characterize the spectral absorption properties of commercially and ecologically important zooplankton species that have the potential to influence ocean color signals, using the PSICAM serial addition method [7]. This work compares the absorption spectra of six keystone species of zooplankton to begin to resolve variability both between and within species of the same population. Further, the impact of each group on simulated remote sensing reflectance (R_{rs}) is presented to begin to explore their impact on ocean color signals. Finally, concentration threshold estimates for detection from satellite data were determined for both Case-1 and Case-2 environments, to investigate the potential utility of satellite derived ocean color products for future identification of surface populations from space. Broadly, this study presents foundational insights into the spectral absorption properties of some key zooplankton groups and lays important groundwork for future research into the potential use of ocean color remote sensing as a tool for identifying and monitoring keystone organisms.

2. Methods

2.1. Zooplankton sampling

The aim of this study was to generate as many absorption spectra of key zooplankton groups as possible. As a result, zooplankton sampling was opportunistically conducted in two locations, at different depths with different sampling nets. A total of 6 different zooplankton species were sampled for this study. The first sampling location was Loch Etive (LE), a regularly sampled sea loch located on the west coast of Scotland. Samples were taken from station RE5, located in the Upper Basin at the deepest part of the loch, at depths of 146 m (Fig. 1(a)) on the 7th March 2022. Samples were collected using a WP2 plankton net with a 200 µm mesh size (Hydro-Bios, GmbH, Germany) from the upper 50 m. Samples were sorted according to species, stored in water from LE and transported back to the laboratory. Here they were stored in a refrigerator at 5°C for a maximum of two days whilst experiments were conducted.

Zooplankton samples were also taken from the northern Norwegian Sea during the SFI Harvest cruise on board the R/V 'Helmar Hanssen' from 7th -14th June 2022 (SFI). Zooplankton samples were taken from different depths across 5 different stations during the cruise (Fig. 1(b)). These

Optics EXPRESS

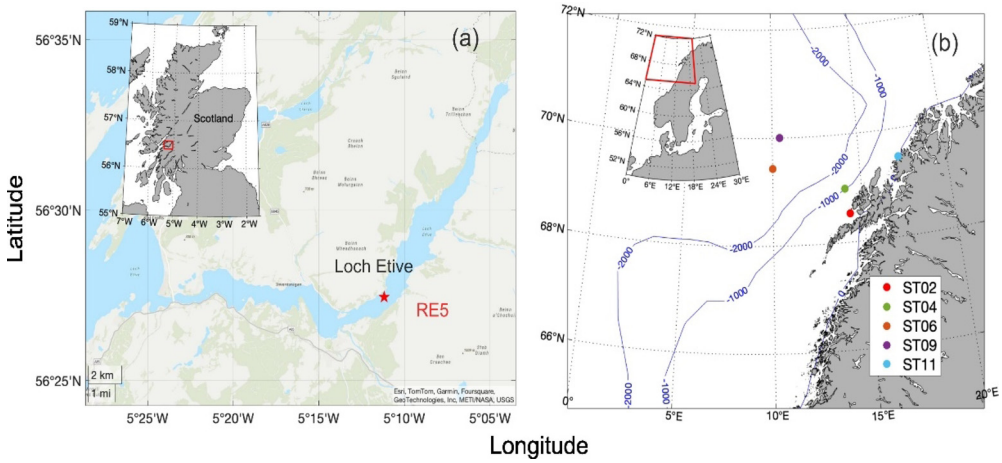

Fig. 1. Map of site that was sampled in (a) Loch Etive on 7th March 2022 and (b) the sites sampled during the June 2022 SFI Harvest cruise in the northern Norwegian Sea.

samples were collected using two types of plankton net: a MultiNet midi (0.25 m^2 opening, 180 µm mesh size, Hydrobios, Germany), as well as a Tucker Trawl (used primarily to collect krill samples), with a mouth opening of 1m^2 and a 1000 µm mesh size (Hydrobios, Germany). Once the samples were collected, the zooplankton were picked and sorted to genus level (and species level where possible). Once samples had been sorted, they were stored in a dark refrigerator at a temperature of 6°C until analysis was conducted. A summary table of all the zooplankton sampled at both sites, as well as their size range (at adult) and sampling location, is presented in Table 1.

Table 1. Summary of all zooplankton species sampled for this study.

Species	Sampling location	Station	Sampling Depth [m]	Date sampled	Number of absorption spectra	Size range of adult [mm]
C. finmarchicus	LE	RE5	50-0	07/03/22	4	2-4
	SFI	ST09	80-0	12/06/22	2	
C. hyperboreus	SFI	ST09	80-0	12/06/22	1	4-7
P. norvegica	LE	RE5	50-0	07/03/22	2	5-11
M. norvegica	SFI	ST11	300	13/06/22	11	22-45
Parathemisto spp.	SFI	ST02, ST04, ST06	30-0	08/06/22-11/06/22	3	6-25
Limacina spp.	SFI	ST02, ST04, ST06	30-0	08/06/22-11/06/22	3	1-3

2.2. Measuring zooplankton absorption

The spectral absorption properties of each zooplankton group were measured in a Point Source Integrating Cavity Absorption Meter (PSICAM) [9,19]. The PSICAM is virtually unaffected by scattering error [9] and is ideally suited for the measurement of samples containing particulate matter (such as zooplankton). The set-up consists of a spherical cavity illuminated with an isotropic light source placed at the centre (Fig. 2(a)). This integrating sphere produces multiple reflections at the cavity walls, resulting in long pathlengths and high measurement sensitivity.

Optics EXPRESS

With the addition of a homogenous, diffuse light source, scattering effects are minimised. The PSICAM measures light intensity at the cavity wall when the cavity is filled with a reference and sample fluid. These irradiances can be converted into spectral absorption coefficients using calculations outlined by Kirk [20] and Leathers et al. [21].

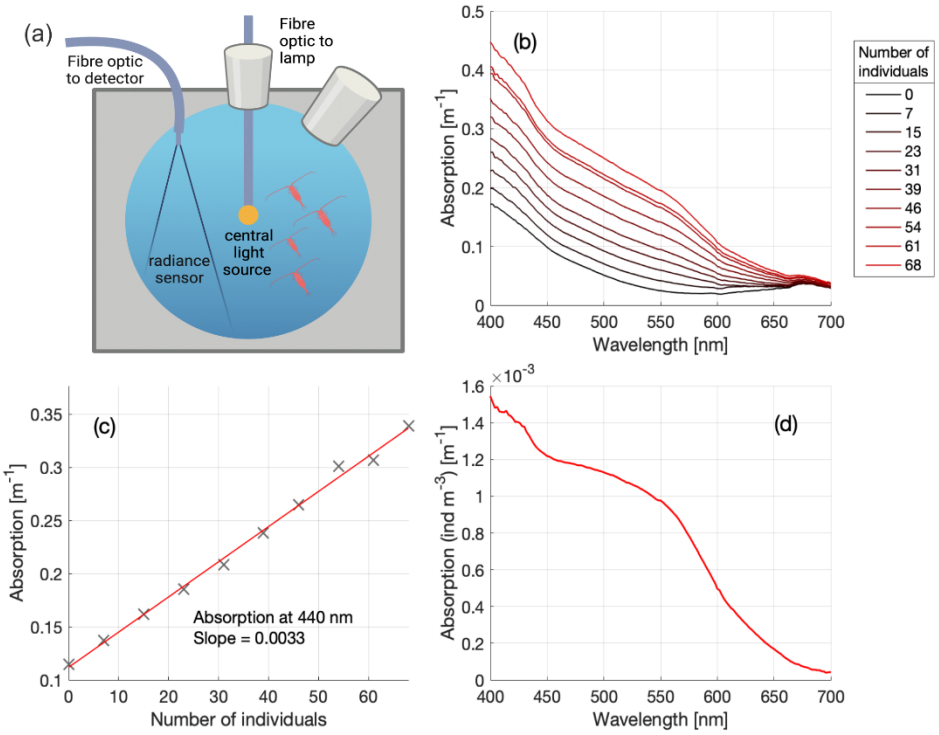

Fig. 2. (a) Schematic of a Point Source Intergrating Cavity Absorption Meter (PSICAM), the instrument used to measure the absorption properties of zooplankton in this study (schematic created in Biorender), as well as (b) an example of the absorption spectra derived from the serial addition experiment of *C. finmarchicus* and (c) associated regression analysis between absorption and number of individuals at 440 nm. The slope of this regression represents the per-individual absorption value at 440 nm. This is divided by the volume of the PSICAM to obtain (d) the concentration specific absorption spectrum for each organism.

The majority of these measurements were conducted using a serial addition method, where at each step of the experiment a number of live zooplankton are sequentially added to a filtered seawater sample (filtered by a 180 µm mesh to remove large particles), with purified Milli-Q water providing a reference measurement. This method was first utilized to measure the spectral absorption of *C. finmarchicus* in Basedow et al. [7]. The number of individuals input at each step was dependent on the size and pigmentation of the organism being measured. Smaller organisms with less pigmentation required more individuals per addition to obtain a signal, whilst larger/more heavily pigmented organisms required fewer. Each organism was added to the seawater sample by hand, to ensure only individuals that were moving and showed no visible sign of stress were selected for the measurement process. Data were corrected for temperature and salinity effects using instrument specific correction factors presented by Lefering [22]. The PSICAM was calibrated throughout the measurement process using Nigrosine solution, following the method outlined in Kirk [20], with corresponding Nigrosine absorption spectra being measured in triplicate using a liquid waveguide capillary cell (LWCC). The PSICAM was thoroughly rinsed after each measurement and bleached after each nigrosine calibration to maintain the reflectivity

Optics EXPRESS

of the cavity walls. The serial addition experiment of an SFI *C. finmarchicus* sample is presented in Fig. 2 as an illustrative example. The number of measurements varied for each organism measured, largely due to sample availability and time constraints associated with handling live samples. Replicate experiments were always conducted on fresh samples. A summary of the number of absorption measurements collected for each zooplankton sample is presented in Table 1.

To obtain a per-individual absorption spectrum for each serial addition, a simple linear regression between the number of individuals and absorption at each wavelength (between 400–700 nm) was conducted. The slope of this relationship provided the per-individual absorption value at each wavelength (see Fig. 2(c) as an example). The spectra were then divided by the volume of the PSICAM to get a concentration-specific absorption spectrum (Fig. 2(d)). The nature of this method, i.e. the use of multiple individuals to obtain one absorption spectrum, accounts for some degree of pigmentation variability within the population to be considered.

With the application of the serial addition method to the krill species *M. norvegica*, some issues were encountered. At certain points throughout the measurement process, the absorption signal would inexplicably jump, leading to erroneously high absorption measurements. This issue did not occur with any of the other organisms measured and was unlikely to be the result of instrumentation instability, as this was regularly checked throughout the measurement process. As these organisms were considerably larger and more mobile than the others measured, their movements may disrupt the uniformity of the light field. It is possible that during the measurement process, one or more of the individuals moved directly under the sensor and/ or light source, resulting in an anomalous jump in absorption. However, as these organisms were so large and pigmented, their absorption signal could be measured on an individual basis. To accommodate this, the data processing procedure was adapted to yield absorption measurements from the attempted serial additions. At each addition, one live organism was added on a step-wise basis

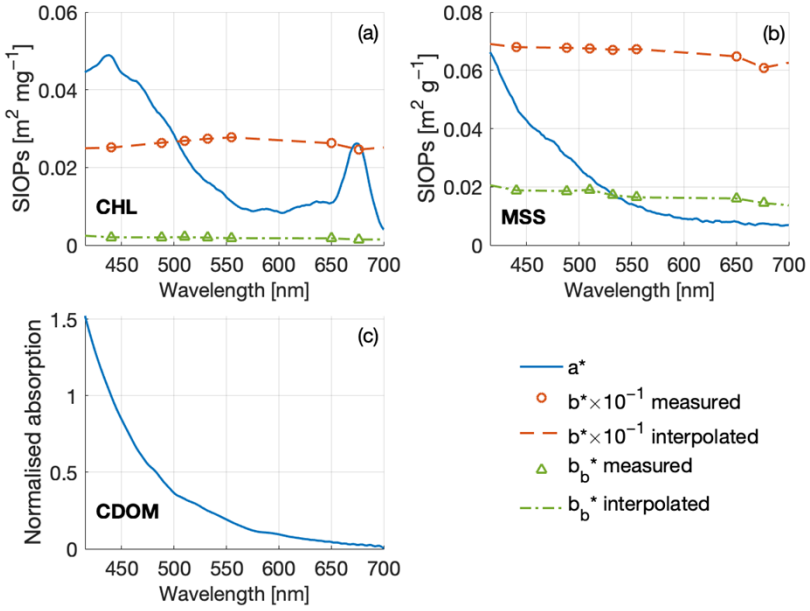

Fig. 3. The SIOP spectra used for the radiative transfer simulations in this study: specific absorption (a*, blue), scattering (b*,orange) and backscattering (b_b*, green) of (a) phytoplankton (CHL), (b) material suspended sediment (MSS) and (c) colored dissolved organic matter (CDOM).

Optics EXPRESS

to filtered seawater. However, instead of regression analysis determining the per-individual absorption at each wavelength, the absorption spectrum at each step in the experiment was subtracted from the spectrum of the previous step, and the erroneous measurements were excluded from analysis.

2.3. Radiative transfer modelling

In order to understand the impact of each zooplankton group on ocean color signals, above surface spectral remote sensing reflectance (R_{rs}) was simulated in Ecolight (version 5.2 Sequoia Scientific Inc, USA), with varying concentrations of each zooplankton group included. The measured absorption spectra were used to represent each zooplankton 'constituent' within the model and was varied linearly with concentration to obtain concentration-specific absorption spectra.

The simulations were conducted using a bio-optical model developed by Lo Prejato et al. [23], which utilizes material specific inherent optical properties (SIOPs) of chlorophyll (including both chlorophyll and non-pigmented algal material) (CHL) (Fig. 3(a)), MSS (Fig. 3(b)) and CDOM (Fig. 3(c)) collected from the Ligurian Sea in March 2009. A detailed description of the data collection and methods can be found in Bengil et al. [24]. To determine the impact of background constituents on zooplankton signals, the simulations were conducted twice for each group measured. The IOPs of the standard constituents were varied to reflect a clear water Case-1 scenario (with only 0.1 mg m^{-3} of CHL) and a moderately Case-2 scenario informed by the conditions in the northern Norwegian Sea when high surface concentrations of the zooplankton *C. finmarchicus* were identified from satellite imagery (1.7 mg m^{-3} of CHL, 0.06 m^{-1} of CDOM and 0.03 gm^{-3} of MSS) [7,8]. Within both scenarios, the concentration of each zooplankton group was varied from 0 to 100,000 individuals m^{-3} (hereafter ind m^{-3}) at the surface (0 m depth), modelled with a homogenous water column and infinite depth. The model was set up with zero cloud cover, a solar zenith angle of 90 °, a windspeed of 7.9 m s^{-1}, a refractive index of 1.34 for seawater, water temperature of 5.5 °C and a salinity of 34 psu. Note that the surface reflectance presented here do not include sun glint effects. Simulations were conducted between 412 nm and 714 nm at 2 nm intervals. Raman scattering was the only form of inelastic scattering included the model, as CHL and CDOM fluorescence were not included.

3. Results

3.1. Zooplankton absorption spectra

The measured absorption spectra of the 6 groups of zooplankton can broadly be divided into astaxanthin rich (AR) species and non-astaxanthin rich (NAR) species (species which don't have high levels of astaxanthin). All of the AR species belonged to the Crustacean subphylum and included advanced developmental stages of the copepod species *C. finmarchicus*, *C. hyperboreus* and *P. norvegica*, as well as the northern krill species *M. norvegica*. To begin to explore the variance of absorption properties between organisms within the same species, *C. finmarchicus* are further divided into an LE population and a northern Norwegian Sea population (SFI). These two sample sites represent very different environmental conditions. LE is a dark, CDOM rich fjord where zooplankton were sampled from a station with a maximum depth of 146 m. Conversely, the SFI populations were sampled off-shelf in the Norwegian Sea, where depths reach 3000 m. Similarly, whilst the carnivorous copepods *P. norvegica* were solely collected from the LE sample site, some of the individuals within the sample were larger and had large dark egg sacs. These were partitioned from the smaller individuals, to begin to explore variability in absorption properties associated with life stage. The spectral absorption properties of each group are represented in Fig. 4. Groups with multiple spectral absorption measurements are represented by the mean (solid line), with the shaded area denoting the standard deviation at each waveband.

Optics EXPRESS

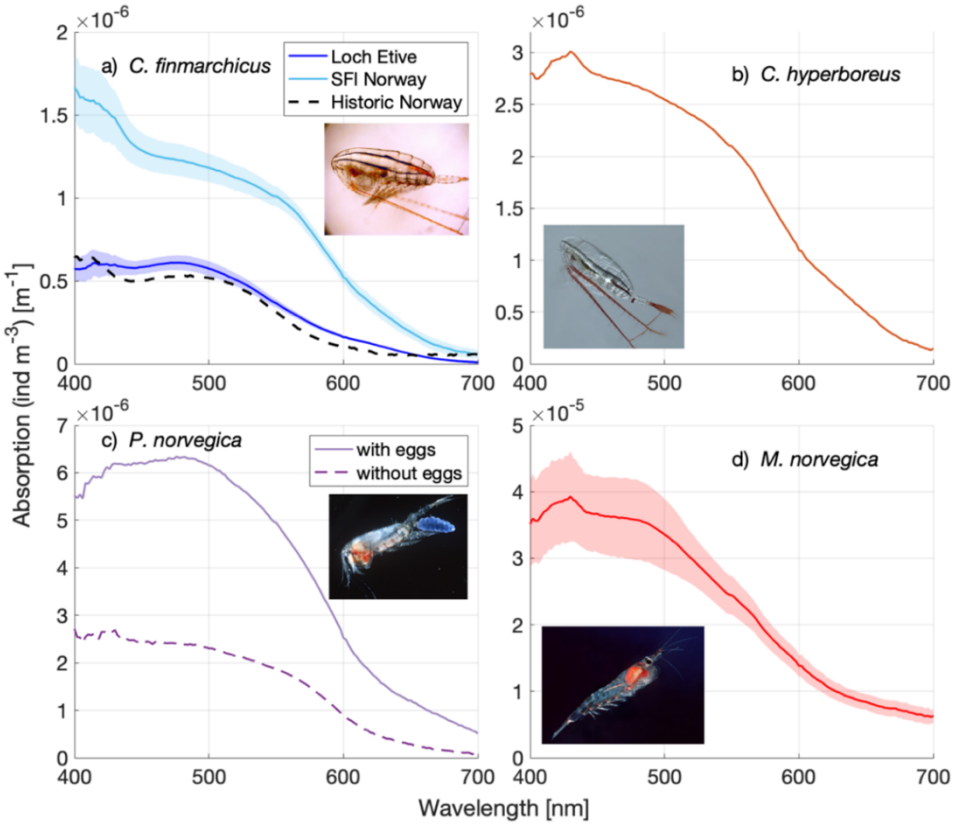

Fig. 4. The absorption spectra of the four astaxanthin rich (AR) species measured in this study: (a) *Calanus finmarchicus* (image source: Michael Bok, CC BY-SA 4.0), (b) *Calanus hyperboreus* (image source: Ross Hopcroft [25] (c) *Paraeuchaeta norvegica* (image source: Jean-François St-Pierre, CC BY-SA 4.0) and (d) *Meganyctiphanes norvegica* (Image source: Uwe Kills, CC BY SA 4.0). For groups with multiple absorption measurements, the average spectrum is presented with a shaded area around it representing 1 standard deviation. Note the y axis scale varies with each subplot, to take into account the order of magnitude difference in absorption between the groups.

All four species appear to have similar spectral absorption properties, with strong absorption in the blue/ green region of the spectrum, peaking at around 486 nm. This peak is characteristic of the pigment astaxanthin [7]. Absorption reduces considerably in the red wavelengths, with most groups showing close to no absorption at 700 nm. The exceptions to this are the krill species *M. norvegica* (Fig. 4(d)) and *P. norvegica* with egg sacs (Fig. 4(c)), both of which absorb in the red. This signal likely originates from the relatively large black eyes of the krill, and the dark eggs associated with the *P. norvegica* group. Despite having similar absorption properties, the shape of the absorption peak does vary slightly between groups, with *C. hyperboreus*, the SFI *C. finmarchicus* and the smaller *P. norvegica* sample showing broader peaks across the blue/ green part of the spectrum relative to the LE *C. finmarchicus*, the *P. norvegica* with eggs and the *M. norvegica* groups. These differences could be driven by the expression of different carotenoid pigments within each group. The spectral magnitude also varies quite considerably between groups. Taking into consideration the y-axis scale on Fig. 4, it is evident that *M. norvegica* have a considerably stronger absorption signal than the other organisms measured. This difference can be attributed to the much larger size of *M. norvegica* individuals (around 20-30 mm) relative

Optics EXPRESS

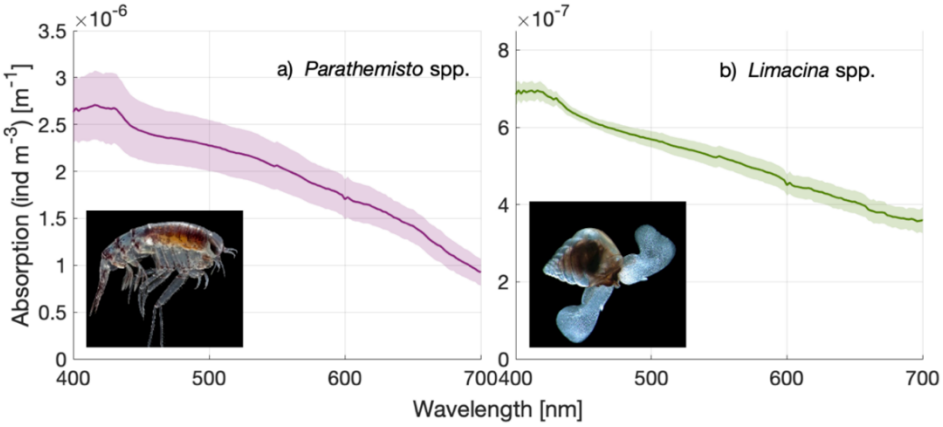

Fig. 5. Absorption spectra of the two non-astaxanthin rich species measured in this study: (a) *Parathemisto* spp. (Image source: Maria Włodarska-Kowalczuk [26]) and (b) *Limacina* spp. (Image source: Ross Hopcroft [27]). For groups with multiple absorption measurements, the average spectrum is presented with a shaded area around it representing 1 standard deviation. Note the y axis scale varies with each subplot, to account for variability between the groups.

to the other organisms (Table 1), resulting in more pigmentation per-individual. Further, the *C. finmarchicus* (Fig. 4(a)) and *P. norvegica* (Fig. 4(c)) results indicate strong variance within populations of the same species. Whilst the LE population of *C. finmarchicus* yielded a very similar spectrum to the historic Norwegian Sea spectrum first measured during the spring 2017 cruise (represented by the black dashed line) [7], it differs quite considerably from the June 2022 Norwegian Sea spectrum measured during the SFI cruise.

The absorption spectra of the two NAR groups, *Parathemisto* and *Limacina* are presented in Fig. 5. Both are characteristically purple to brown in color and appear to have very similar absorption features. For both species, absorption reduces from the blue to red region of the spectrum, but their absorption spectra are fairly featureless. Spectral magnitude does vary between the two species, with *Parathemisto* individuals producing a stronger absorption signal than *Limacina* (note y axis scales), which can again be attributed to their size difference (Table 1).

3.2. Modelled impact of zooplankton on remote sensing reflectance signals

The modelled impact of each AR group on spectral R_{rs} is presented in Fig. 6. These spectra were all modelled using a CHL concentration of 1.7 mg m^{-3} a CDOM concentration of 0.06 m^{-1} and an MSS concentration of 0.03 g m^{-3}, as these were the concentrations measured *in situ* during the 2017 Sea Patches cruise, when high surface abundances of *C. finmarchicus* were identified using satellite imagery [7,8]. Overall, all of the AR organisms have a broadly similar effect of reducing R_{rs} spectral magnitude, most notably in the blue/ green part of the spectrum. This is a natural consequence of modelling their optical impact as only involving additional absorption. Unsurprisingly, the northern krill (*M. norvegica*) (Fig. 6(f)) have the most significant impact on modelled reflectance signals across the spectrum, resulting in lower reflectance in the blue relative to the red with the addition of 100,000 ind m^{-3}.

Comparison between the LE (Fig. 6(a)) and the SFI (Fig. 6(b)) *C. finmarchicus* shows that the SFI population impacts reflectance signals to a greater degree than the LE organisms. Similarly, the impact of the two *P. norvegica* life stages varies quite significantly, with the larger individuals with eggs (Fig. 6(d)) reducing the reflectance signals more than the smaller organisms (Fig. 6(e)). These results suggest that difference in pigmentation and life stage between individuals within the same population can alter their impact on R_{rs} signals quite considerably.

Optics EXPRESS

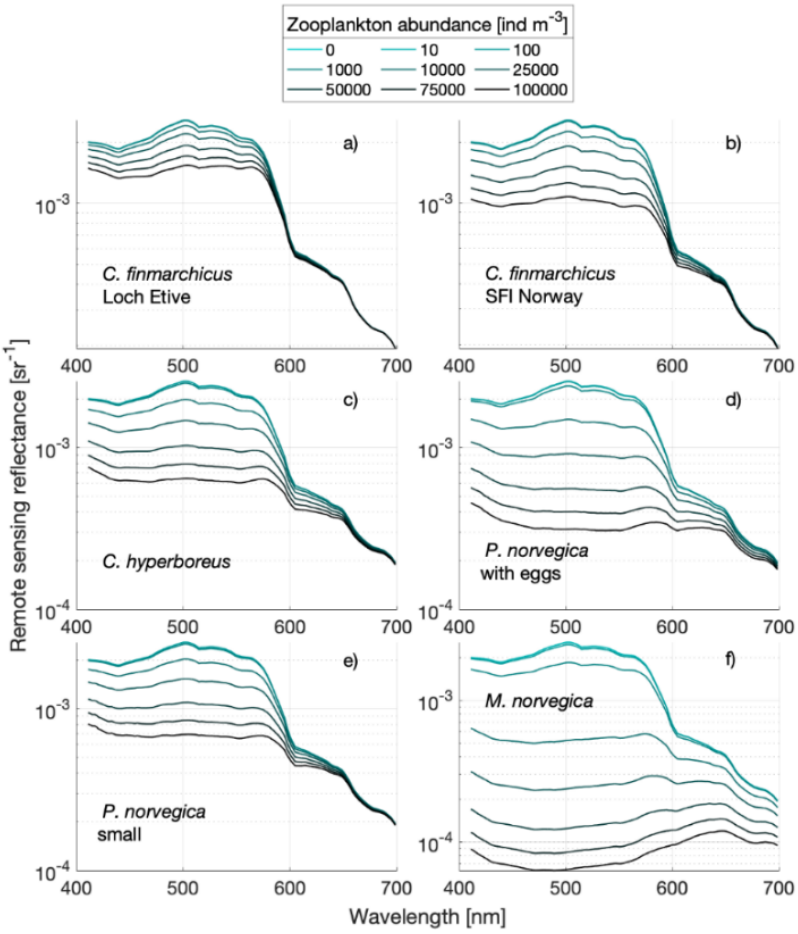

Fig. 6. Modelled remote sensing reflectance spectra with increasing concentrations of (a, b) *Calanus finmarchicus*, (c) *Calanus hyperboreus*, (d, e) *Paraeuchaeta norvegica*, (f) *Meganyctiphanes norvegica*.

The impact of the NAR species (Fig. 7) is broadly similar to that of the AR species. However, as both *Limacina* and *Parathemisto* absorb across the spectrum, their impact on reflectance signals is greater in the red wavelengths relative to the AR species (with the exception of *M. norvegica* and *P. norvegica* with eggs, both of which have black features that absorb in this region).

3.3. Remote detection of zooplankton from satellite ocean color signals

To detect zooplankton from ocean color, their impact on reflectance signals must be characterized and quantified. This can be achieved by numerically comparing an initial spectrum without a zooplankton component to spectra with the inclusion of certain known concentrations of each organism (Fig. 6 and 7). This initial spectrum represents a standard spectrum that may be found in a typical Case-2 environment. Thus, the degree of change introduced by each zooplankton group will provide understanding of how their signal is likely to deviate from a standard bio-optical model. Following a similar method to that outlined in McCarry et al. [8], this anomaly can provide a target for remote identification.

Optics EXPRESS

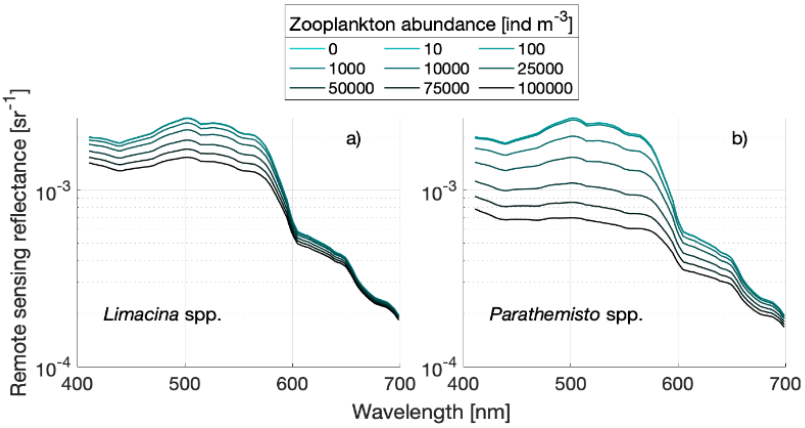

Fig. 7. Modelled remote sensing reflectance spectra with increasing concentrations of (a) *Limacina* spp. and (b) *Parathemisto* spp.

This study aims to assess the potential for use of satellite derived ocean color products in remote detection of zooplankton. Therefore, satellite sensor capabilities must be taken into account when determining the impact of these organisms on ocean color signals. Most notably, the majority of easily accessible satellite datasets have multispectral resolution. An example of this is the MODIS Aqua sensor, which collects data at 10 wavebands within the visible spectrum. In a study conducted by Hu et al. [28] R_{rs} uncertainty estimates associated with 7 of these wavebands (412 nm, 443 nm, 488 nm, 531 nm, 547 nm, 667 nm and 678 nm) were presented, providing an estimate of variability expected from MODIS data at these wavebands. These uncertainties were calculated using mean absolute percentage error/ difference (MAPD), for 5 different chlorophyll concentrations (between 0.03-0.2 mg m^{-3}) that broadly represented Case-1 waters. MAPD is regularly used within the literature to estimate uncertainty associated with satellite products. Hu et al. also included data from both the North Atlantic and South Pacific, in order to encapsulate regions with different aerosol influences, as atmospheric correction is one of the largest sources of uncertainty within satellite derived ocean color data. This work provides a benchmark to compare with zooplankton-induced anomaly, to ascertain the concentration of organisms required to have an identifiable impact on R_{rs} signals.

3.3.1. Waveband selection for identification of zooplankton-associated anomaly

In order to obtain the strongest anomaly signal possible from the measured zooplankton groups, it is important to determine which wavebands should be involved in the spectral comparison process. From the modelled data presented above (Figs. 6 and 7), it is apparent that most of the zooplankton groups are having a more considerable influence in the blue/ green relative to the red end of the spectrum. Therefore, it is possible that the inclusion of wavebands across the visible spectrum will lead to a dilution of the zooplankton-associated anomaly. Despite this, it is important to include as much spectral information as possible to ensure good discrimination between different optical constituents.

To determine the optimal number of wavebands for the spectral comparison exercise, the MAPD between the initial Case-2 R_{rs} spectrum and the spectrum including 10,000 ind m^{-3} of each zooplankton group was calculated. As a first attempt, this comparison was conducted 7 times for each group and each time the amount of spectral information included in the comparison was increased. Thus, the first MAPD analysis was conducted using the 412 nm waveband only, the second with 412 nm and 443 nm and so on until all 7 wavebands with associated uncertainty estimates were included. The averaged results for both the AR species and NAR species are

Optics EXPRESS

presented in Fig. 8. From this analysis, it is evident that the inclusion of 5 wavebands in the spectral comparison process is optimal for the identification of zooplankton associated anomaly, as the highest MAPD scores were achieved when 5 wavebands were compared. The wavebands included were 412 nm, 443 nm, 488 nm, 531 nm and 547 nm. With the addition of the red wavebands (667 nm and 678 nm) the MAPD scores were reduced, suggesting that the inclusion of wavebands where zooplankton are having a minimal impact may lead to a masking effect of the anomaly signal. This effect would likely be more significant with the application of this method to satellite data, where instrument noise and atmospheric correction effects can further mask the zooplankton associated signal.

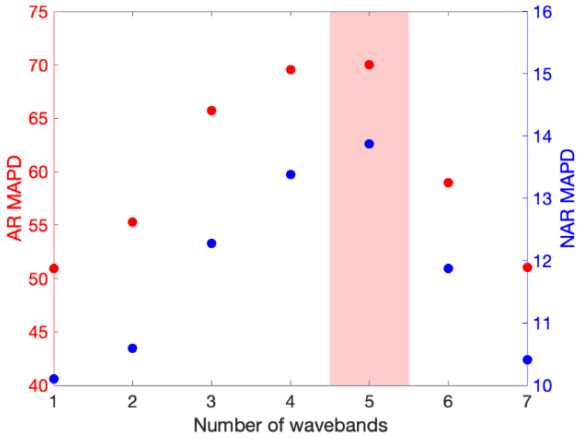

Fig. 8. The average mean absolute percentage difference (MAPD) of the reflectance spectra generated by 10,000 ind m^{-3} of the astaxanthin rich (AR) and non-astaxanthin rich (NAR) species when compared to a standard Case-2 spectra with no zooplankton included. This analysis was conducted multiple times, with increasing numbers of wavebands included in the comparison. As indicated by the red shaded area, the inclusion of 5 wavebands produced the strongest zooplankton-associated signal for both groups.

3.3.2. Concentration thresholds for detection of zooplankton from satellite imagery

Concentration thresholds for the detection of each zooplankton group were determined using the MAPD spectral comparison approach. The comparison was conducted using the 5 wavebands discussed above for optimal zooplankton associated anomaly detection. The modelled spectra produced from discrete concentrations (from 0 to100,000 ind m^{-3}) of each zooplankton group were compared to the initial spectrum without any zooplankton included (representing a standard bio-optical spectrum). Initial R_{rs} spectra modelled from a moderately Case-2 scenario (1.7 mg m^{-3} of CHL, 0.06 m^{-1} CDOM and 0.03 g m^{-3} of MSS) (Figs. 6 and 7) and an open water Case-1 scenario (with 0.1 mg m^{-3} CHL only) were compared, to analyse the effect of background constituents on zooplankton detection. For each concentration, the MAPD from the initial spectrum was calculated, and the exact concentration at which the MAPD exceeded the determined threshold was linearly interpolated from the modelled MAPD results.

The anomaly threshold was determined using Hu et al. [28] spectral R_{rs} uncertainty analysis. For the 5 wavebands included in the spectral comparison, MAPD estimates ranged from 1.6% (443 nm, 0.03 mg m^{-3} of chlorophyll), to 18.8% (547 nm, 0.15 mg m^{-3} of chlorophyll). Therefore, as a first attempt, a nominal threshold in the middle of this range was chosen (10%). Thus, the concentration at which each zooplankton group exceeds this 10% MAPD is the concentration at

Optics EXPRESS

which the anomaly signal generated by each zooplankton group is strong enough to be identified from ocean color data.

The concentration thresholds for each zooplankton group in both Case-1 and Case-2 waters is presented in Table 2, to 2 significant figures. Results indicate that all zooplankton groups studied exceeded the detection threshold within the simulated concentration ranges. It is evident from the results that the background constituents within the water column influences the threshold of detection, with considerably higher concentrations required to influence optical signals in Case-2 waters relative to Case-1. Further, the concentration thresholds vary quite considerably both between and within species. For example, the LE population of *C. finmarchicus* require the highest concentrations of individuals at 20,000 ind m^{-3} and 3,200 ind m^{-3} for Case-2 and Case-1 waters respectively. However, the SFI population required less than half of that in both Case-1 and 2 waters (8,700 and 1,300 ind m^{-3}). Similarly, the *P. norvegica* individuals with egg sacs required far lower concentrations (310 ind m^{-3} and 1,800 ind m^{-3} for Case-1 and Case-2 waters respectively) than the smaller individuals within the same population (750 ind m^{-3} and 4,600 ind m^{-3}). Notably, *M. norvegica* require the lowest concentrations out of all the species measured, at only 330 ind m^{-3} required to reach the threshold in Case-2 waters. Again, this difference is likely due to the larger size of these organisms producing a stronger absorption feature on a per-individual basis.

Table 2. Concentrations of each zooplankton group required to reach the threshold of detection (10% MAPD), modelled in both a Case-1 and Case- 2 environment.

Astaxanthin content	Species	C1 concentrations [ind m^{-3}]	C2 concentrations [ind m^{-3}]
Astaxanthin rich	LE *C. finmarchicus*	3200	20000
(AR)	SFI *C. finmarchicus*	1300	8700
	C. hyperboreus	670	4200
	P. norvegica (with eggs)	310	1800
	P. norvegica (small)	750	4600
	M. norvegica	50	330
Non- astaxanthin rich	*Limacina* spp.	2900	18000
(NAR)	*Parathemisto* spp.	730	4500

4. Discussion

4.1. Comparison of the spectral absorption properties of six zooplankton groups

This study presents the spectral absorption properties of six ecologically and commercially important zooplankton groups. Unlike the Basedow et al. [7] study, this work does not present a *in situ* match up exercise with satellite data, thereby allowing greater flexibility to extend zooplankton sampling efforts beyond the surface layer. This facilitated the collection of many more absorption spectra, providing insights into variability both between and within species. The absorption signals of the AR species are spectrally similar, with astaxanthin appearing to be the dominant driver of absorption. Absorption is generally high in the blue/ green part of the spectrum, with a peak at around 480 nm which decreases to near zero at the red end. Minor differences in the shape of the absorption peak may be attributed to the presence/ absence of other carotenoid pigments within each group. Despite this, there is considerable variation in the magnitude of absorption between different species, which appears broadly related to the size of individuals within each population. Most notably, the northern krill species *M. norvegica* produced a per-individual absorption spectrum an order of magnitude stronger than the other species (Fig. 4). These organisms are considerably larger than the others measured in this study (Table 1) and therefore contain more absorbing pigment. Further, unlike the other AR species,

Optics EXPRESS

these organisms produce a non-negligible absorption signal in the red end of the spectrum, which may be attributed to their large black eyes. Generally, these organisms proved challenging to measure, occasionally causing erroneous jumps in absorption measurements. This is likely due to their significant size and mobility disrupting the uniformity of the light field within the cavity. In this study, these erroneous spectra were removed from analysis. However, in order to minimize this interference for future work, sampled individuals could be partially sedated to reduce movement and/ or measurements could be conducted in a PSICAM with a larger cavity where their movement would be less disruptive.

With the partition of *C. finmarchicus* into the LE and SFI population, intra-species variability can begin to be examined. Results indicate that spectral absorption properties, most notably spectral magnitude, can vary quite considerably between organisms within the same species. The absorption spectra obtained from the LE population in 2022 was very similar to that of the historic Norwegian Sea spectra collected during the Sea Patches cruise in 2017 [7]. Conversely, the 2022 SFI Harvest Norwegian Sea spectra had a stronger absorption signal with a broader peak (Fig. 4(a)). The primary driver of variability in pigment expression between individuals of the same species or population is unknown, largely due to the plasticity of this functional trait [17]. In general, more pigmented individuals tend to be more successful than their uncolored counterparts, due to the variety of benefits that carotenoid pigments provide. One of the leading hypotheses for pigment accumulation in copepods is that carotenoids provide photoprotection for individuals and prevent degradation of their lipid sacs [17]. A factor that may explain the apparent variability between the LE and SFI organisms is the considerable difference in habitat that each of these populations experience. *C. finmarchicus* in the Norwegian Sea exhibit traditional population dynamics, where they swarm at the surface to feed in the spring/ summer and return to the depths in the winter months for diapause [29]. Conversely, LE *C. finmarchicus* typically remain at depths of around 50 m and feed off the CDOM rich, dark fjord waters. Variability in their exposure to solar radiation, as well as the nutritional quality of their food source, could be contributing to these marked differences in pigmentation. However, this does not explain the apparent variability within Norwegian Sea populations sampled in April/ May 2017 (historic measurement) and June 2022 (SFI measurements). In the context of this study, the more pigmented population were those sampled in the northern Norwegian Sea in June 2022. During this time of year, these organisms are exposed to increased UV radiation, as the region experiences 24-hour daylight in the summer months. Conversely, the LE population never experience 24-hour daylight and the 2017 Norwegian Sea spectrum was collected in April/ May, when the region still experiences 4-5 hours of darkness. It is possible that this increased exposure to UV radiation resulted in an increase in photoprotective pigments within the SFI population. However, this cannot be concluded on the basis of a few absorption measurements alone and it is likely that a variety of factors are influencing the variability in this highly plastic functional trait. Therefore, more work on characterising the spatio-temporal patterns in pigmentation expression both between and within species is required.

Additionally, the difference between the two sub-samples of *P. norvegica* indicate that life stage may have an impact on the absorption properties of some zooplankton species, as spectral magnitude (and to a lesser extent spectral shape) varied quite considerably between the smaller individuals and the larger females with egg sacs. In general, these results illustrate the importance of considering both environmental factors and variability associated with life stage when attempting remote optical detection of zooplankton species. Further, the results demonstrate the suitability of the PSICAM serial addition method as a means to quantify variability in zooplankton color. As this has been identified as a key functional trait in copepods that can provide an indicator of population fitness [17], continued use of this method will directly provide information that has potential to aid in the monitoring of ecosystem health. Thus, more work to

Optics EXPRESS

fully characterize the variability documented in this study is required, in order to better understand these organisms and inform modelling efforts for zooplankton identification.

The considerable influence of astaxanthin on the spectral properties of the AR species points to the requirement of a general astaxanthin-based algorithm for the remote optical detection of these species. Despite small differences in spectral shape, it is likely that any detection method identifying the absorption signals presented above may produce 'false positives' with the presence of any astaxanthin rich species in the surface waters. As a result, an understanding of the assemblage composition within the region of interest would likely be required before remote detection can be attempted. With understanding of *in situ* populations and measurements of the target species absorption properties, a detected astaxanthin signal could be converted into species abundances.

Unsurprisingly, the spectral absorption properties of the NAR species varied from that of the AR species. Most notably, these organisms had a flatter spectrum and no discernable absorption peak. Generally, both species absorbed across the visible spectrum, with a slight decrease in absorption from the blue to the red wavelengths. This could make remote identification of these organisms through ocean color signals difficult. These relatively featureless absorption spectra could be mis-identified as other optically important constituents, e.g. CDOM or detritus, which have similar absorption properties to these organisms (Fig. 3(c)). Thus, with the currently available multi-spectral data, a lot of *in situ* information and validation would be required to confidently identify these organisms from satellite imagery, which largely negates the utility of remote detection. However, the advent of National Aeronautics and Space Adiminstration's (NASA) new hyperspectral Plankton Aerosol Clod and Ocean Ecosystem (PACE) satellite may provide the spectral resolution required to improve discrimination between optically similar constituents such as these.

The impact of both the AR and NAR groups on modelled reflectance signals was very similar. The inclusion of increasing concentrations of zooplankton acted to draw down reflectance signals, especially in the blue/ green region of the spectrum. Some of the zooplankton groups (*M. norvegica*, *Parathemisto* spp.) also noticeably reduced reflectance at the red wavelengths. This similarity is a natural consequence of modelling the optical impact of all zooplankton groups as a function of absorption only. This work provides a robust first attempt at examining the optical impact of these organisms because as Davies et al. [6] theoretically demonstrated, 'particles' of this size are likely to most significantly influence the bulk absorption properties of the water column. Despite this, it is important to characterize the influence of these organisms on the scattering and backscattering of the water column. Unfortunately, current *in situ* IOP measurement systems are biased towards smaller, more abundant particles, largely due to their relatively small sample volumes. The PSICAM serial addition method adopted in this study provides a means to overcome this issue with regards to absorption, but there are currently no alternatives for measuring the scattering and backscattering properties of these organisms. Thus, future work is required, both to develop new methods of *in situ* IOP sensing that captures the impact of larger particles such as zooplankton, and the exploration of alternative methods (both theoretical and practical) to estimate the impact of these organisms on bulk scattering and backscattering properties.

4.2. Establishing the utility of satellite derived ocean color for the remote detection of zooplankton

To establish the utility of satellite ocean color data as a means for remote identification of these organisms, the modelled signal generated by up to 100,000 ind m^{-3} of each zooplankton group was compared to an initial reflectance signal without the addition of any organisms. This provided a measure of anomaly for each zooplankton group, which indicates how far their reflectance signal diverges from a standard Case-2 signal. The greater the anomaly signal, the

Optics EXPRESS

more distinguishable these organisms are from ocean color data. The McCarry et al. [8] study used a similar methodology to identify the zooplankton species *C. finmarchicus* from ocean color imagery in the northern Norwegian Sea. The enhanced RGB (eRGB) color co-ordinate of each pixel (derived from the spectral R_{rs} at 443 nm, 488 nm and 555 nm) was compared to a look-up table of simulated eRGB co-ordinates that represented a standard Case-2 model. Regions where the standard Case-2 model did not provide optical closure (i.e. a high degree of anomaly) were resolved using a specialized Case-2 model with the inclusion of *C. finmarchicus* absorption. From this, concentration maps of *C. finmarchicus* were generated.

Comparison of the anomaly signals generated by both the AR and NAR groups with the incorporation of different wavebands indicated that a 5 waveband comparison produced the strongest anomaly signals. With the inclusion of red bands 6 and 7 (667 nm and 678 nm), the anomaly signal decreased. As all of these organisms had a more considerable impact in the blue/green, the inclusion of red wavebands appeared to dilute the zooplankton associated anomaly. This illustrates the importance of carefully considering the wavebands utilized in spectral anomaly and matching methods and points to the requirement of targeted waveband approaches that best highlight the impact of the target organism. This will become particularly critical in the age of hyperspectral satellite data, where there is an abundance of spectral information to analyse. Whilst these data will provide a powerful tool to resolve more fine-scale optical features, indiscriminate inclusion of all available wavebands across the spectrum may serve to decrease the likelihood of identifying optically anomalous signals.

Detection thresholds for each organism were calculated to determine concentrations required to produce a detectable signal from ocean color. A general observed trend was that larger organisms produced stronger absorption signals, which in turn required lower densities to surpass the threshold of detection. This finding corroborates the findings of Davies et al. [6], which illustrated that the relative contributions of large particles to absorption was highly sensitive to changes in the Junge slope. It was found that increasing the relative concentration of large particles (i.e. lifting the Junge slope) resulted in a stronger absorption signal. As zooplankton are ubiquitous in the global ocean, the density thresholds were calculated using simulated reflectance spectra in two background scenarios broadly representing a Case-1 environment (0.1 mg m-3 of CHL), and a Case-2 environment (1.7 mg m-3 of CHL, 0.03 g m-3 of MSS and 0.06 m-1 of CDOM). From this, it is evident that the optical complexity of the region of interest will influence the likelihood of zooplankton detection. For every group measured in this study, far lower concentrations were required to reach the detection threshold in the Case-1 environment relative to the Case-2 simulations. For example, only 3,200 ind m^{-3} of the LE population of *C. finmarchicus* were required to reach the detection threshold in Case-1 waters, which contrasts with the 20,000 ind m^{-3} required in Case-2 environments. This considerable disparity highlights the importance of considering the optical complexity of the region of interest when attempting remote detection of these organisms.

Concentration thresholds required for detection in Case-2 waters were on the high end of *in situ* observations, especially for *C. finmarchicus* populations (for example, see literature review of *C. finmarchicus* aggregations in the Gulf of Maine by Ross et al. [30]). This may suggest that concentrations this high do not often naturally occur in the ocean. However, dense surface swarms that far exceed 20,000 ind m^{-3} have previously been recorded *in situ* [15,31] with the study by Wishner et al. [31] recording concentrations of up to 331,000 ind m^{-3} within a visibly red surface patch. Further, the McCarry et al. [8] study remotely estimated *C. finmarchicus* concentrations of up to 180,000 ind m^{-3} in the northern Norwegian Sea, which was an order of magnitude greater than the concentrations derived from *in situ* sampling during the same time period (maximum of 16,000 ind m^{-3}). One hypothesis put forward to explain this deviation was animal evasion behavior. These organisms can swim, and often undergo diel vertical migration that spans hundreds of meters. Therefore, it is possible that these organisms can swim to avoid

Optics EXPRESS

capture, leading to a potential under estimation of these populations. In fact, a recent study conducted in the same region by Bandara et al. [32], found concentrations of 165,000 ind m^{-3} at 10 m depth, with the use of an acoustic sensor attached to a free floating sailbouy. As well as this, Dunn et al. [33] demonstrated, through the comparison of data derived from a broadband echosounder mounted on an autonomous surface vehicle with net and trawl surveys in the northern Norwegian Sea, that population estimates of copepods derived from the net samples were lower than the acoustic estimates. This difference was higher for the more mobile zooplankton groups and was attributed to avoidance bias. It is therefore possible that *in situ* net sampled concentration estimates are not fully resolving surface populations and concentrations of these organisms could be higher than the literature currently reflects. This points to a requirement for less invasive *in situ* sampling techniques to ground truth satellite observations. As well as this, traditional zooplankton sampling techniques could be underestimating *in situ* populations simply due to the patchy distributions of these organisms. Many traditional methods are designed to sample one station at a time, broadly representing one point in the ocean. Therefore, if a large aggregation of zooplankton were located just out of the stations' sampling range, these organisms would not be represented in population estimates, despite potentially contributing significantly to the total zooplankton abundances in this region.

The concentrations of *C. finmarchicus* required to produce a strong enough signal to be identified through satellite imagery varied considerably between the two populations modelled. The LE *C. finmarchicus* required 11,300 ind m^{-3} more than that of the SFI population to reach the anomaly threshold of 10%. As the majority of individuals within these samples were stage CV, this difference is likely driven by various environmental factors, as opposed to life stage. This therefore emphasizes the importance of prior understanding of both the region of interest, as well as the zooplankton assemblage being targeted when developing ocean color detection techniques. This difference is considerable enough to suggest the possibility of multiple *C. finmarchicus* models that can be used depending on the region/ time of study and the assemblage being targeted.

Further, comparison of the density thresholds derived from the two different samples of *P. norvegica* show a similar story of variation. More than double the number of small *P. norvegica* were required to reach the concentration threshold relative to the mature *P. norvegica* individuals with eggs. This difference is likely driven by the size difference between the two life stages and illustrates the importance of considering the life stages of a target species when attempting remote identification to ensure greater accuracy of concentration estimates. This was a first attempt at quantifying the effect of zooplankton demography on pigmentation and absorption properties, and more work needs to be done to better understand this phenomenon.

M. norvegica required by far the smallest concentration of individuals in order to reach the detection threshold, which is likely due to their considerable size relative to the other organisms measured in this study. This is a positive result in terms of potential for remote identification of krill swarms through ocean color. Nicol [10,34] recorded small scale, visually identifiable surface swarms of *M. norvegica* in the Bay of Fundy that reached densities of 770,000 ind m^{-3}. These concentrations were remotely determined from aerial photography and contrasted with minimally invasive *in situ* 'bag sampled' concentration estimates, which reached a maximum of 41,000 ind m^{-3}, as well as traditional net sampled concentrations of only 6 ind m^{-3}. Taking into account these abundances, it is possible that natural populations could reach the maximum determined detection threshold of 330 ind m^{-3} and therefore be identified remotely. Additionally, the difference in concentration estimates derived from the three techniques used in Nicol [29] further demonstrates the potential for animal evasion to influence concentration estimates. The remote (helicopter camera) and minimally invasive (bag sampling) methods yielded concentration estimates that were orders of magnitude greater than the more invasive net sampling method. Other studies have also identified and investigated krill evasion behaviour, demonstrating that

Optics EXPRESS

these highly mobile organisms, in particular larger members of the population, can evade net capture [35–37]. The evasion behaviour of krill was also found to be more significant at the surface, where there is lots of light and krill can visually detect sampling nets [36]. This further highlights the need for development of non-invasive *in situ* sampling techniques to provide surface concentration estimates that are free from evasion bias and are more representative of natural concentrations.

A lot of the interest regarding remote detection of krill is concentrated on the Southern Ocean, which supports some of the largest krill fisheries in the world [4] and *in situ* population monitoring is difficult due to the challenging conditions of the region. In the Southern Ocean, *E. superba* are the dominant krill species and are generally larger than their northern counterparts. Therefore, it is possible than even lower densities would be required to produce an identifiable signal through ocean color. The range of *E. superba* swarm densities vary considerably in the literature, with acoustic estimates in the Scotia Sea ranging from 3-81 ind m^{-3} but reaching up to 1650 ind m^{-3} [38]. However, visual estimates have exceeded these values by an order of magnitude, ranging between 25,000 to 64,000 ind m^{-3} [39]. Consequently, it is likely that some of these high concentration events may be visible through satellite imagery. The results presented here for *M. norvegica* are a first attempt at understanding the absorption properties of krill, and provide a strong indication that remote sensing of krill swarms from ocean color signals is feasible. However, more work is needed to characterise krill absorption properties, especially for the Antarctic species *E. superba*, which are of significant biological and economic interest globally, and are larger than the krill species studied here.

Whilst the determined concentration thresholds appear to fall within the range of *in situ* observations for *C. finmarchicus* [15,30], *C. hyperboreus* [14] and *M. norvegica* [34], *in situ* concentration estimates of *Limacina* species [40], *Parathemisto* species [41] and *P. norvegica* [42] appear to be lower, on the order of 100 ind m^{-3} or less. This would suggest that these organisms do not naturally reach concentrations that can impact ocean color. However, the literature on these organisms is sparse relative to the continually studied calanoid copepods and krill. As well as this, concentrations have been derived using invasive net sampling techniques. Again, work on *in situ* abundance estimates using non-invasive sampling techniques are required to provide accurate ground-truthing, especially for more understudied zooplankton groups.

Further, it is important to remember that contribution to absorption properties is not the only factor that will influence the likelihood of detection of these organisms. As well as being concentrated enough to produce a signal, aggregations will have to cover a significant spatial scale. For example, the spatial resolution of the MODIS Aqua satellite sensor is 1 km^2. If these organisms aggregate on more localised scales, then they will likely not be resolved through satellite imagery. In addition, all of the other restrictions associated with satellite detection apply here, including light availability, cloud cover and optical depth. For the remote detection of more localized swarms in areas that are frequently covered by cloud, cameras attached to drones or aircrafts may provide a suitable alternative. Whilst these methods do not offer the same spatio-temporal resolution that satellite data provides, the spatial coverage achieved by these methods will exceed that of ship-based measurements. Detection will further depend on population dynamics of target groups. The ocean color remote sensing window of opportunity occurs during the spring/ summer months where these organisms inhabit the surface waters to graze. In particular, phytoplankton spring blooms trigger mass zooplankton swarming events, which will likely considerably increase their contribution to ocean color signals. Conversely, many populations of zooplankton (including copepods and krill) go into diapause in the deep ocean during the winter months and therefore will not be detected from ocean color data. Thus, the behaviour, life cycle and location of these populations will also influence the likelihood of remote detection.

Optics EXPRESS

5. Conclusions

This study presents an initial analysis of the absorption properties of six ecologically and commercially important zooplankton groups, and the evaluation of their potential impact on ocean color remote sensing signals. The findings highlight the spectral similarity of four of these groups (3 copepod species and northern krill), with features that appear to be driven by the carotenoid pigment astaxanthin. This spectral similarity suggests the requirement of an astaxanthin- based detection method for the remote identification of these organisms, which can then be converted into animal abundance estimates with prior knowledge of *in situ* zooplankton assemblages. Conversely, the two NAR species (amphipods and sea butterflies) produced a relatively featureless absorption spectrum, which poses a challenge for the remote detection of these organisms under current multi-spectral resolution constraints. However, with the recent launch of NASA's hyperspectral satellite PACE, there is greater scope for remote detection in the future. The results also highlight considerable variability in absorption properties within populations of the same species, which underscores the importance of considering both spatio-temporal factors and assemblage composition when attempting remote optical detection of zooplankton. Whilst this study provides a first attempt at characterising this variability, more work is required to explore these features and the drivers.

Modelling efforts revealed that increasing concentrations of all zooplankton groups can have considerable impacts on reflectance signals, particularly in the blue/ green region of the visible spectrum. It was demonstrated that careful waveband selection is required in the development of remote sensing algorithms that are tailored to zooplankton detection. This study also presented concentration thresholds for detection of these organisms in both Case-1 and Case-2 waters, which fell within the range of *in situ* concentrations for three species that have previously been recorded within the literature.

Generally, this study provides evidence that supports the utility of ocean color remote sensing as a method to monitor the wide-scale surface distributions of zooplankton populations. However, more work is required to characterise the variability in absorption properties both between and within zooplankton groups, as well as the development of methods to estimate scattering and backscattering properties, to obtain a complete optical profile of these organisms. Further, continued development of remote sensing algorithms is required to better facilitate detection and quantification of these populations from satellite data.

Funding. Natural Environment Research Council (NE/P00573X/1); Norges Forskningsråd (287043 STRESSOR project).

Acknowledgments. The authors would like to thank the captain and crew of the R/V *Helmer Hanssen* for their professional support during cruise operations.

Disclosures. The authors declare no conflict of interest.

Data availability. Data underpinning this publication are openly available from the University of Strathclyde KnowledgeBase at [43].

References

1. Z. L. R. Botterell, P. K. Lindeque, R. C. Thompson, *et al.*, "An assessment of the ecosystem services of marine zooplankton and the key threats to their provision," Elsevier B.V. **63**, 101542 (2023).
2. D. K. Steinberg and M. R. Landry, "Zooplankton and the Ocean Carbon Cycle," Annu. Rev. Mar. Sci. **9**(1), 413–444 (2017).
3. S. H. Jónasdóttir, A. W. Visser, K. Richardson, *et al.*, "Seasonal copepod lipid pump promotes carbon sequestration in the deep North Atlantic," Proc. Natl. Acad. Sci. **112**(39), 12122–12126 (2015).
4. Marine Zooplankton Colloquium 2, "Future marine zooplankton research- a perspective," Mar. Ecol. Prog. Ser. **222**, 297–308 (2001).
5. L. Ratnarajah, R. Abu-Alhaija, A. Atkinson, *et al.*, "Monitoring and modelling marine zooplankton in a changing climate," Nat. Commun. **14**(1), 564 (2023).
6. E. J. Davies, S. L. Basedow, and D. McKee, "The hidden influence of large particles on ocean colour," Sci. Rep. **11**(1), 3999 (2021).

Optics EXPRESS

7. S. L. Basedow, D. McKee, I. Lefering, *et al.*, "Remote sensing of zooplankton swarms," Sci. Rep. **9**(1), 686 (2019).
8. C. L. McCarry, S. L. Basedow, E. J. Davies, *et al.*, "Estimating Surface Concentrations of *Calanus finmarchicus* Using Standardised Satellite-Derived Enhanced RGB Imagery," Remote Sens (Basel) **15**(12), 2987 (2023).
9. R. Röttgers, W. Schönfeld, P.-R. Kipp, *et al.*, "Practical test of a point-source integrating cavity absorption meter: the performance of different collector assemblies," Appl. Opt. **44**(26), 5549–5560 (2005).
10. S. Nicol, "Population structure of daytime surface swarms of the euphausiid Meganyctiphanes norvegica in the Bay of Fundy," Mar. Ecol. Prog. Ser. **18**, 241–251 (1984).
11. J. R. Dadon, "Annual cycle of Limacina retroversa in Patagonian waters," 1990.
12. H. B. Bigelow, *Plankton of the offshore waters of the Gulf of Maine*. 1926.
13. W. R. Siegfried, "Observations on the Amphipod *Parathemisto Gaudichaudi* (Guer.) off the West Coast of South Africa," Zoologica Africana **1**(2), 339–352 (1965).
14. S. Kwasniewski, H. Hop, S. Falk-Petersen, *et al.*, "Distribution of *Calanus* species in Kongsfjorden, a glacial fjord in Svalbard," J Plankton Res **25**(1), 1–20 (2003).
15. N. Weidberg, N. Santana Hernandez, A. H. H. Renner, *et al.*, "Large scale patches of *Calanus finmarchicus* and associated hydrographic conditions off the Lofoten archipelago," Journal of Marine Systems **227**, 103697 (2022).
16. H. K. Schminke, "Entomology for the copepodologist," Journal of Plankton Research **29**, i149–i162 (2007).
17. L. Vilgrain, F. Maps, S. Basedow, *et al.*, "Copepods' true colours: pigmentation as an indicator of fitness," Ecosphere, 2023.
18. C. Manno, N. Morata, and R. Primicerio, "*Limacina retroversa's* response to combined effects of ocean acidification and sea water freshening," Estuar Coast Shelf Sci **113**, 163–171 (2012).
19. R. Röttgers, C. Häse, and R. Doerffer, "Determination of the particulate absorption of microalgae using a point-source integrating-cavity absorption meter: Verification with a photometric technique, improvements for pigment bleaching, and correction for chlorophyll fluorescence," Limnol Oceanogr Methods **5**(1), 1–12 (2007).
20. J. T. O. Kirk, "Point-source integrating-cavity absorption meter: theoretical principles and numerical modelling," Appl. Opt. **36**(24), 6123–6128 (1997).
21. R. A. Leathers, T. V. Downes, and C. O. Davis, "Analysis of a point-source integrating-cavity absorption meter," Appl. Opt. **39**(33), 6118–6127 (2000).
22. I. Lefering, "Characterisation of a Point-Source Integrating Cavity Absorption Meter for applications in optical oceanography," University of Strathclyde, Glasgow, 2016.
23. M. Lo Prejato, D. McKee, and C. Mitchell, "Inherent Optical Properties-Reflectance Relationships Revisited," J Geophys Res Oceans **125**(11), JC016661 (2020).
24. F. Bengil, D. McKee, S. T. Beşiktepe, *et al.*, "A bio-optical model for integration into ecosystem models for the Ligurian Sea," Prog Oceanogr **149**, 1–15 (2016).
25. R. Hopcroft, "Calanus hyperboreus," ArcoDiv , (2024), http://www.arcodiv.org/watercolumn/copepod/Calanus_hyperboreus.html.
26. M. Włodarska-Kowalczuk, "Parathemisto spp," DWARF , (2024), https://www.iopan.gda.pl/projects/Dwarf/species_gallery/crustacea.html.
27. R. Hopcroft, "Limacina spp.," ArcoDiv , (2024), http://www.arcodiv.org/watercolumn/pteropod/Limacina_retroversa.html.
28. C. Hu, L. Feng, and Z. Lee, "Uncertainties of SeaWiFS and MODIS remote sensing reflectance: Implications from clear water measurements," Remote Sens Environ **133**, 168–182 (2013).
29. K. S. Tande and C. C. E. Hopkins, "Ecological investigations of the zooplankton community of balsfjorden, northern norway: The genital system in *Calanus finmarchicus* and the role of gonad development in overwintering strategy," Mar. Biol. **63**(2), 159–164 (1981).
30. C. H. Ross, J. A. Runge, J. J. Roberts, *et al.*, "Estimating North Atlantic right whale prey based on *Calanus finmarchicus* thresholds," Mar. Ecol. Prog. Ser. **703**, 1–16 (2023).
31. R. D. Kenney and K. F. Wishner, "The South Channel Ocean Productivity EXperiment," Continental Shelf Research **15**(4-5), 373–384 (1995).
32. K. Bandara, S. L. Basedow, G. Pedersen, *et al.*, "Mid-summer vertical behavior of a high-latitude oceanic zooplankton community," Journal of Marine Systems **230**, 103733 (2022).
33. M. Dunn, G. Pedersen, S. L. Basedow, *et al.*, "Inverse method applied to autonomous broadband hydroacoustic survey detects higher densities of zooplankton in near-surface aggregations than vessel-based net survey," Can. J. Fish. Aquat. Sci. **80**(3), 451–467 (2023).
34. S. Nicol, "Shape, size and density of daytime surface swarms of the euphausiid Meganyctiphanes norvegica in the Bay of Fundy," 1986. [Online]. Available: https://academic.oup.com/plankt/article/8/1/29/1607998
35. I. Everson and D. G. Bone, "Effectiveness of the RMT8 System for Sampling Krill (Euphausia superba) Swarms," Polar Biology **6**, 83–90 (1986).
36. H. J. Hill, P. N. Trathan, J. P. Croxall, *et al.*, "A comparison of Antarctic krill *Euphausia superba* caught b y nets and taken by macaroni penguins *Eudyptes chrysolophus*: evidence for selection?" Mar. Ecol. Prog. Ser. **140**, 1–11 (1996).
37. A. S. Brierley, "A comparison of Antarctic euphausiids sampled by net and from geothermally heated waters: insights into sampling bias," Polar Biol. **22**(2), 109–114 (1999).
38. G. A. Tarling and S. Fielding, "Swarming and Behaviour of Antarctic Krill," in *Biology and Ecology of Antarctic Krill*, V. Siegel, Ed., Springer, 2016, pp. 279–319. [Online]. Available: http://www.springer.com/series/10290
39. W. M. Hamner and P. P. Hamner, "Behavior of Antarctic krill (*Euphausia superba*): schooling, foraging, and antipredatory behavior," Can. J. Fish. Aquat. Sci. **57**(S3), 192–202 (2000).
40. P. Kacprzak, A. Panasiuk, J. Wawrzynek, *et al.*, "Distribution and abundance of pteropods in the western Barents Sea," Oceanol Hydrobiol Stud **46**(4), 393–404 (2017).

Optics EXPRESS

41. H. Auel and I. Werner, "Feeding, respiration and life history of the hyperiid amphipod *Themisto libellula* in the Arctic marginal ice zone of the Greenland Sea," J Exp Mar. Biol. Ecol **296**(2), 183–197 (2003).
42. A. Yamaguchi and T. Ikeda, "Abundance and population structure of three mesopelagic *Paraeuchaeta* species (Copepoda: Calanoida) in the Oyashio region, western subartic Pacific Ocean with notes on their carcasses and epizoic ciliates," Plankton Biology and Ecology **48**(2), 1 (2001).
43. C. L.. McCarry and D.. McKee, "Data repository for: Determination of zooplankton absorption spectra and their potential contribution to ocean color," University of Strathclyde KnowledgeBase 1.0 2024, https://doi.org/10.15129/bea8ea3f-3a4d-4d33-a0d7-5cd16b108362.